Consistent Relationship between Field-Measured Stomatal Conductance and Theoretical Maximum Stomatal Conductance in C_3 Woody Angiosperms in Four Major Biomes

Journal Item

Int. J. Plant Sci. 181(1):000–000. 2020.

1058-5893/2020/18101-00XX$15.00 DOI: 10.1086/706260

CONSISTENT RELATIONSHIP BETWEEN FIELD-MEASURED STOMATAL CONDUCTANCE AND THEORETICAL MAXIMUM STOMATAL CONDUCTANCE IN C_3 WOODY ANGIOSPERMS IN FOUR MAJOR BIOMES

Michelle Murray,[1,*] Wuu Kuang Soh,* Charilaos Yiotis,* Robert A. Spicer,†,‡ Tracy Lawson,§ and Jennifer C. McElwain*

*Department of Botany, School of Natural Sciences, Trinity College Dublin, Dublin 2, Ireland; †Xishuangbanna Tropical Botanical Garden, Chinese Academy of Sciences, Menglun, Yunnan, China; ‡School of Environment, Earth and Ecosystem Sciences, Open University, Milton Keynes, United Kingdom; and §School of Biological Sciences, University of Essex, Wivenhoe Park, Colchester, Essex, United Kingdom

Guest Editor: Juliana Medeiros

Premise of research. Understanding the relationship between field-measured operating stomatal conductance (g_{op}) and theoretical maximum stomatal conductance (g_{max}), calculated from stomatal density and geometry, provides an important framework that can be used to infer leaf-level gas exchange of historical, herbarium, and fossil plants. To date, however, investigation of the nature of the relationship between g_{op} and theoretical g_{max} remains limited to a small number of experiments on relatively few taxa and is virtually undefined for plants in natural ecosystems.

Methodology. We used the g_{op} measurements of 74 species and 35 families across four biomes from a published contemporary data set of field-measured leaf-level stomatal conductance in woody angiosperms and calculated the theoretical g_{max} from the same leaves to investigate the relationship between g_{op} and g_{max} across multiple species and biomes and determine whether such relationships are widely conserved.

Pivotal results. We observed significant relationships between g_{op} and g_{max}, with consistency in the g_{op}:g_{max} ratio across biomes, growth habits (shrubs and trees), and habitats (open canopy and understory subcanopy). An overall mean g_{op}:g_{max} ratio of 0.26 ± 0.11 (mean ± SD) was observed. The consistently observed g_{op}:g_{max} ratio in this study strongly agrees with previous hypotheses that an ideal g_{op}:g_{max} ratio exists.

Conclusions. These results build substantially on previous studies by presenting a new reference for a consistent g_{op}:g_{max} ratio across many levels and offer great potential to enhance paleoclimate proxies and vegetation-climate models alike.

Keywords: biome, habitat, operational stomatal conductance, theoretical maximum stomatal conductance, woody angiosperms.

Online enhancements: appendix tables and figure.

Introduction

Stomatal conductance is the exchange of carbon dioxide for photosynthesis and water vapor via transpiration through microscopic pores called stomata on the areal parts of plants, principally the leaf surface. Diffusion of water vapor through stomata is 1.6 times that of carbon dioxide; therefore, transpirational water loss from the leaf is a costly but unavoidable trade-off between plants' photosynthetic gain and productivity (Farquhar and Sharkey 1982) and their instantaneous water use efficiency (ratio of rate of transpiration to CO_2 uptake; Katul et al. 2009; Manzoni et al. 2011; Buckley and Schymanski 2014; Franks et al. 2015).

Stomata are highly sensitive to fluctuating environmental conditions such as light, temperature, and CO_2. The stomatal pore is surrounded by two guard cells that are highly sensitive to environmental signals such as changes in light intensity, temperature and humidity, soil moisture and nutrient status, and internal guard cell and mesophyll signals. Resulting changes in turgor pressure in the guard cells adjust the stomatal opening to regulate gaseous exchange, maximize CO_2 uptake, and minimize water loss (Farquhar and Sharkey 1982; Schulze et al. 1994; Hutjes et al. 1998; Hetherington and Woodward 2003;

[1] Author for correspondence; email: mnmurray40@gmail.com.

Manuscript received June 2019; revised manuscript received September 2019; electronically published December 5, 2019.

Mott 2009; Franks et al. 2013; Lawson and Blatt 2014; McAusland et al. 2016). Through their short-term critical opening-closing response to rapid environmental change, as well as the longer-term developmental downregulating in response to rising atmospheric CO_2, stomata have potential to greatly influence ecosystem function and the global carbon and hydrologic cycles. Therefore, they play a pivotal role in Earth system and plant-climate feedbacks (Hetherington and Woodward 2003; Gedney et al. 2006; Betts et al. 2007; Berry et al. 2010; Keenan et al. 2014; Schlesinger and Jasechko 2014; Lin et al. 2015; Ukkola et al. 2015; Engineer et al. 2016; Li et al. 2016) and are critical in determining vegetation response to environmental change (Leakey et al. 2009; Medlyn et al. 2011).

Stomatal conductance, referred to here as "operational stomatal conductance" (g_{op}; McElwain et al. 2016*b*), is a function of the stomatal density (D) and the depth and degree of openness of the stomatal pore (pa_{max}) in response to internal and environmental signals (Berry et al. 2010; Drake et al. 2013). The theoretical maximum stomatal conductance (g_{max}) is calculated from measurements of the stomatal density and geometry according to a diffusion equation (eq. [1] in "Material and Methods"; Parlange and Waggoner 1970; Franks and Beerling 2009). These same stomatal traits ultimately determine g_{op} (Franks and Beerling 2009), yet the nature of the relationship between g_{op} and g_{max} remains largely unquantified beyond a small number of growth chamber and greenhouse studies (Franks et al. 2009; Dow et al. 2014; McElwain et al. 2016*b*).

It has been observed that measured g_{op} in field conditions rarely achieves the maximum theoretical g_{max} limits, as defined by leaf anatomical traits (Körner 1995; Lawson and Morison 2004; Dow and Bergmann 2014). Furthermore, because it is a purely theoretical measurement, theoretical g_{max} is usually greater than the observed g_{op} by a large degree (Sack and Buckley 2016). This disparity has propelled many areas of botanical research into establishing the basis for this (Franks et al. 2009; Dow et al. 2014; McElwain et al. 2016*b*). For example, studies have explored the extreme variability in stomatal distribution across a leaf surface (Casson and Gray 2008) and how stomatal development and, therefore, stomatal density are heavily influenced by environmental conditions, particularly light (Lake et al. 2001; Lomax et al. 2009) and CO_2 (Woodward 1987; McElwain and Chaloner 1995; Woodward and Kelly 1995; Wagner et al. 1996). Alternatively, the mismatch between g_{op} and g_{max} might be due to the short-term behavioral responses of stomata to minimize transpiration and increase water use efficiency by rapidly reducing their aperture, particularly when evaporative demands are high during drought conditions (Buckley 2005; Katul et al. 2012; Kollist et al. 2014). In addition, over the longer term, g_{max} of a leaf can be altered via changes in size and density in response to protracted drought (Franks et al. 2009, 2015) and/or rising atmospheric carbon dioxide concentrations (Woodward 1987; Ainsworth and Rogers 2007; Franks and Beerling 2009; Lammertsma et al. 2011; Gray et al. 2016). This, in turn, imposes constraints on g_{op} (McElwain et al. 2016*b*). The sheer diversity of species-specific g_{max} and g_{op} responses to abiotic factors and their relationship to one another also prompts us to ask whether a consistent relationship between g_{max} and g_{op} exists. A coordinated trade-off between physiological (g_{op}) and anatomical (g_{max}) control of stomatal conductance has been suggested (Haworth et al. 2013), implying that, if there is coordination, defining a relationship between theoretical g_{max} and physiological g_{op} should be possible. Studies have observed that measured g_{op} is between 20% and 25% of theoretical g_{max}, or in other words, the $g_{op}:g_{max}$ ratio is between 0.2 and 0.25 (Franks et al. 2009, 2014; Dow et al. 2014; McElwain et al. 2016*b*). It has been speculated that this is an ideal level of g_{op}, at which stomata are enabled to respond rapidly to environmental flux by opening or closing as conditions dictate (Franks et al. 2012; Dow et al. 2014).

Over the past 10 years, experiments to determine a reliable relationship between g_{op} and g_{max}, or the $g_{op}:g_{max}$ ratio, have yielded broadly consistent results (Dow et al. 2014; Franks et al. 2014; McElwain et al. 2016*b*); however, these studies have been taxonomically limited and rarely included both measured g_{op} and calculated theoretical g_{max} parameters from the same leaves. The aim of this study was to advance our current understanding of the nature of the relationship between g_{op} and g_{max} across multiple species and biomes to determine whether such relationships are widely conserved. More simply put, we asked whether theoretical g_{max}, which is calculated from stomatal anatomy according to the diffusion equation (eq. [1]; Parlange and Waggoner 1970; Franks and Beerling 2009), is a good predictor of g_{op} measured in the field.

We explored the relationship between g_{op} and g_{max} by measuring g_{op} in a wide range of woody angiosperm species in natural ecosystems and then calculating g_{max} from the same leaves on which the g_{op} measurements were taken to establish the nature of the relationship at biological and ecological levels. Therefore, we tested the relationship across many species, plant growth habits (trees and shrubs), habitats (open canopy and understory subcanopy), and biomes (boreal forest, temperate rain forest, tropical rain forest, and tropical seasonal [moist] forest). If we can establish consistency in the nature of the relationship between g_{op} and g_{max}, this would be valuable for historical herbarium studies and deep-time fossil studies because it would allow estimation of physiological stomatal conductance from observations of anatomical stomatal traits. It would also have an important application for climate and Earth system models in which g_{op} can be estimated from the stomatal traits and, in turn, open up the possibility of studying vegetation feedbacks on the hydrologic cycle.

Material and Methods

Biome and Species Selection

For this study, we used a published field data set of stomatal conductance measurements of C_3 woody angiosperm species from seven biomes called STraits (Murray et al. 2019). We chose the following four out of the seven biomes included in the STraits data set for our current study on the basis that they spanned wide geographic, climatic, and species ranges and are the least well represented in the literature: boreal forest, temperate rain forest, tropical seasonal (moist) forest, and tropical rain forest. We selected 74 species from a total 136 species included in the STraits data set across these biomes (Murray et al. 2019; table 1). Based on the APG IV system of flowering plant classification (APG et al. 2016), our study covers 35 woody angiosperm families and 16 orders, all of which are from the Eudicot clade, which includes the Rosid and Asterid clades. Phylogenetic coverage in this study excludes the basal angiosperm Magnoliids,

the Chloranthales, gymnosperms, monocots, and ferns (APG et al. 2016). One species, *Sambucus racemosa*, occurred in both the boreal forest and the temperate rain forest and was therefore counted as two separate species occurrences, resulting in 75 separate species analyzed (table 1).

Leaf-Level Operational Stomatal Conductance Data

The term "operational stomatal conductance" (g_{op}) used here refers to stomatal conductance as it performs under natural field conditions, following the definition of McElwain et al. (2016*b*). The g_{op} data used in this study are taken from the published STraits data set of Murray et al. (2019). In Murray et al. (2019), stomatal conductance measurements were obtained by the author using an SC-1 steady-state leaf porometer (Decagon Devices, Pullman, WA) over the course of three summer growing seasons between 2013 and 2015, when atmospheric CO_2 concentrations ranged from 396.5 to 400.8 ppm. Measurements were made on the abaxial surface of sun leaves located at the canopy edge or, in the case of naturally occurring understory shrub species, on the abaxial surface of leaves exposed to sun flecks. Mean species g_{op} was calculated from an average total of 12 g_{op} measurements per species (i.e., a single g_{op} measurement taken from one leaf of each of three individuals on three or four consecutive days). This yielded a total 854 measurements on 243 individual leaves (table 1). Measurements were taken between 0830 and 1400 hours at each site under ambient environmental conditions to capture natural day-to-day variability in photosynthetically active radiation (PAR), temperature, and vapor pressure deficit (VPD), a modification of the variance protocol described in McElwain et al. (2016*b*). Detailed methods are available in Murray et al. (2019).

All mean conductance values reported in Murray et al. (2019) were subsequently corrected using a relationship established between stomatal conductance measurements taken by porometry and measurements on the same individuals taken by infrared gas analysis (IRGA).

Measurement of Morphological Traits and Calculation of Theoretical g_{max}

The same 243 leaves on which g_{op} was measured were used for measurement of stomatal morphology (density and size) and for calculation of theoretical g_{max}. A leaf section of 1-cm^2 area was cut from approximately the same location on the leaf where g_{op} measurements were made, yielding a total 243 leaf sections. These were fixed abaxial side up on glass slides without mounting medium and gently secured with a cover slip and tape. Six photomicrographs per leaf section were captured using a Leica DFC300 FX digital color camera mounted on a Leica DM2500 microscope with a ×20 objective lens (×200 magnification; Leica Microsystems, Wetzlar, Germany). Visualization of the stomatal anatomy of most species was achieved via autofluorescence of stomatal complexes under epifluorescence using a range of excitation fluorescence filters (green: 500–570 nm; yellow and orange: 570–610 nm). In the very few instances in which epifluorescence did not yield clear images, leaf epidermal impressions were made by applying clear nail varnish to the abaxial leaf surface of each leaf, approximately where g_{op} measurements were taken. The resulting epidermal impression was then peeled off the leaf using clear Sellotape, transferred directly to microscope slides, and photomicrographed under transmitted light. Leaves on which stomata were obscured by dense trichomes, thick cuticle wax, and/or papillae that could not easily be removed and leaves with stomata not clearly visible under microscopy were not included in the study. Micrographs were generated using Auto-Montage Pro Syncroscopy software (Synoptics, Frederick, MD). A 0.09-mm^2 grid and scale bar were superimposed on each micrograph using AcQuis (ver. 4.0.1.10, Syncroscopy, Cambridge, UK). Stomatal density was estimated using the Cell Counter in ImageJ version 1.49 software (http://imagej.nih.gov/ij) following Poole and Kürschner (1999). Stomatal dimensions—pore length (μm) and guard cell width (μm)—were measured on 10 open stomata randomly selected from the six photomicrographs of each species using ImageJ and converted to meters for g_{max} calculation. Calculations of theoretical g_{max} were then made using the following equation (Parlange and Waggoner 1970; Franks and Beerling 2009):

$$g_{max} = \frac{(d_w/v) \cdot D \cdot pa_{max}}{pd + (\pi/2) \cdot \sqrt{(pa_{max}/\pi)}}, \quad (1)$$

where d_w, diffusivity of water vapor at 25°C (0.0000249 m^2 s^{-1}), and v, molar volume of air (0.0224 m^3 mol^{-1}), are constants; D is stomatal density (m^{-2}); pa_{max} constitutes maximum stomatal pore area (m^2) calculated as an ellipse (Lawson et al. 1998) using stomatal pore length (m) as the long axis and l/2 as the short axis; and pd is stomatal pore depth (m), assumed to be equivalent to the width of one fully turgid guard cell (Franks and Beerling 2009*b*).

Because the dried leaves for this study were not rehydrated by any means, it is possible that leaf area reduced in some species because of shrinkage caused by the drying process (Blonder et al. 2012). The degree of leaf shrinkage varies with plant functional type (PFT; Blonder et al. 2012). We tested for shrinkage in the two PFTs in this study—woody angiosperm evergreen and deciduous—by applying the correction mean shrinkage suggested by Blonder et al. (2012) for these PFTs of 15% for evergreen leaves and 27% for deciduous leaves to the individual leaf stomatal morphological (guard cell width and pore length) and density measurements. We then calculated the new g_{max} (table S1; tables S1–S8 are available online). It is worth noting that the mean area shrinkage for evergreen types is also the reported mean for all woody species (15%; Blonder et al. 2012). A Kruskal-Wallis test for equal medians determined no significant difference between the g_{max} used in this study and the g_{max} calculated from the applied shrinkage factors (table S1). Therefore, all analysis was carried out using g_{max} calculated from the original uncorrected stomatal morphological and density data.

Statistical Analysis

All statistical analysis was carried out using IRGA-corrected species mean g_{op} (as outlined above). Each species mean g_{op} value in a given biome was weighted against the total number of individual g_{op} measurements for that biome according to the following:

$$n \text{ species } g_{op}/n \text{ biome } g_{op} \cdot \text{species } g_{op},$$

Table 1

Mean (± SD) Stomatal Conductance, Stomatal Density (*D*), and Stomatal Geometry Data

Biome	Species	Family	Leaves (*n*)	g_{op} (*n*)	*D* (mm^{-2})	Pore length (μm)	Pore depth (μm)	pa_{max} (μm^{-2})	g_{max} (mmol m^{-2} s^{-1})	g_{op} (mmol m^{-2} s^{-1})	g_{op} : g_{max}
BF	*Alnus alnobetula*	Betulaceae	4	16	158 ± 6.1	9.3 ± .4	6.1 ± .3	34.2 ± 2.7	488 ± 21.6	128 ± 5.2	.26
BF	*Amelanchier alnifolia*	Rosaceae	3	12	128 ± 8.4	16 ± .6	5.4 ± .4	100.4 ± 7.8	922 ± 102.2	170 ± 3.8	.18
BF	*Betula neoalaskana.*	Betulaceae	3	12	153 ± 25.2	17 ± 2.7	6.3 ± .7	115.6 ± 36.7	1127 ± 253.7	131 ± 3.5	.12
BF	*Linnaea borealis*	Caprifoliaceae	4	16	403 ± 34.6	6.2 ± .7	7.8 ± .7	15.3 ± 3.5	553 ± 103.4	94 ± 5.2	.17
BF	*Menziesia ferruginea*	Ericaceae	3	12	72 ± 6.5	14.9 ± .1	6 ± .2	86.6 ± 1.3	445 ± 43.5	131 ± 1.9	.29
BF	*Oplopanax horridus*	Araliaceae	3	12	90 ± 11.8	14.3 ± 1.1	5.6 ± .4	81 ± 12.1	553 ± 133.1	150 ± 4.1	.27
BF	*Populus balsamifera*	Salicaceae	3	12	142 ± 34.3	18.1 ± 1.8	6.9 ± .3	129.2 ± 24.7	1077 ± 158.9	217 ± 4.6	.2
BF	*Populus tremuloides*	Salicaceae	4	16	138 ± 20.4	17.4 ± 1.6	7.2 ± 1.4	119.7 ± 23	1011 ± 287.6	232 ± 7.4	.23
BF	*Ribes laxiflorum*	Grossulariaceae	4	15	109 ± 26.4	11.1 ± 1.1	6.4 ± .8	48.7 ± 9.1	423 ± 64.5	109 ± 2.8	.26
BF	*Sambucus racemosa*	Adoxaceae	3	8	65 ± 14.8	17.1 ± 3	12.6 ± 2.5	117 ± 38.4	350 ± 117.8	201 ± 2.6	.57
BF	*Shepherdia canadensis*	Elaeagnaceae	3	5	143 ± 21.5	8 ± .4	7.9 ± .1	25.4 ± 2.4	301 ± 54.1	114 ± .8	.38
BF	*Sorbus scopulina*	Rosaceae	5	20	137 ± 34.2	17.7 ± 3.9	7.2 ± 1.2	127.1 ± 55.3	966 ± 126.4	221 ± 7.3	.23
BF	*Viburnum edule*	Adoxaceae	4	16	84 ± 4.9	15.2 ± 1.1	6.8 ± 1	91.1 ± 13.4	511 ± 48.4	143 ± 5.4	.28
TRF	*Alnus rubra*	Betulaceae	3	9	296 ± 37.2	7.9 ± .3	7.2 ± .3	24.2 ± 2	630 ± 69.7	146 ± 4	.23
TRF	*Arbutus menziesii*	Ericaceae	3	9	138 ± 25.2	16.6 ± 3.3	10.9 ± .6	111.1 ± 41.5	767 ± 276.6	209 ± 3.6	.27
TRF	*Arctostaphylos columbiana*	Ericaceae	3	9	157 ± 1.2	9.3 ± .6	11.8 ± .5	34.3 ± 4.4	324 ± 36.4	149 ± 2	.46
TRF	*Baccharis pilularis*	Asteraceae	3	7	94 ± 11.6	10.4 ± .7	11 ± 1.1	42.3 ± 5.8	242 ± 30	97 ± 2	.4
TRF	*Berberis nervosa*	Berberidaceae	3	9	94 ± 14.5	8.8 ± .8	6.8 ± .4	30.7 ± 5.8	250 ± 31.2	49 ± 1.7	.2
TRF	*Frangula purshiana*	Rhamnaceae	3	9	248 ± 18.8	8.8 ± 1.7	6.7 ± .9	30.9 ± 12.1	656 ± 93.5	176 ± 4.4	.27
TRF	*Garrya elliptica*	Garryaceae	3	9	130 ± 3.2	10.9 ± 1.5	9.5 ± .7	46.8 ± 13	395 ± 71	199 ± 1.8	.5
TRF	*Gaultheria shallon*	Ericaceae	3	6	223 ± 31	9.2 ± .5	8.7 ± .3	33.4 ± 3.6	552 ± 91.5	93 ± 4	.17
TRF	*Gaylussacia baccata*	Ericaceae	3	9	120 ± 20.6	7.7 ± 1.8	4.1 ± .6	24.2 ± 10.8	350 ± 143	57 ± 2.2	.16
TRF	*Holodiscus discolor*	Rosaceae	3	9	141 ± 16.7	7.6 ± .2	7 ± .3	22.9 ± 1	295 ± 34.7	82 ± 2.4	.28
TRF	*Lonicera hispidula*	Caprifoliaceae	3	9	200 ± 11.6	9.9 ± .4	5.5 ± .3	38.6 ± 3.3	719 ± 70.6	63 ± 1.7	.09
TRF	*Lonicera involucrata*	Caprifoliaceae	3	7	250 ± 14	11.1 ± .3	6.3 ± .3	48.7 ± 2.2	999 ± 49.8	132 ± 3.6	.13
TRF	*Myrica californica*	Myricaceae	3	9	196 ± 18.5	8.6 ± 1.2	9.2 ± .8	29.2 ± 8.2	409 ± 49	164 ± 1.9	.4
TRF	*Rhododendron macrophyllum*	Ericaceae	3	9	112 ± 22.4	11 ± 1.3	7.3 ± 0	47.7 ± 10.7	414 ± 140.2	39 ± 2.6	.09
TRF	*Ribes sanguineum*	Grossulariaceae	3	9	154 ± 36.8	10.5 ± .6	6.3 ± 1.1	43.3 ± 5.1	568 ± 162.9	132 ± 2.7	.23
TRF	*Rubus parviflorus*	Rosaceae	3	9	202 ± 44.5	7.6 ± 1.2	4.2 ± .5	22.8 ± 7.3	543 ± 85	132 ± 3.1	.24
TRF	*Rubus spectabilis*	Rosaceae	3	8	264 ± 52.4	7.9 ± 1.2	3.8 ± .1	24.6 ± 7.5	782 ± 123.1	139 ± 5.9	.18
TRF	*Salix hookeriana*	Salicaceae	3	9	273 ± 35.7	11.2 ± .6	6 ± .3	49.4 ± 5.2	1124 ± 135.3	273 ± 3.7	.24
TRF	*Sambucus racemosa*	Adoxaceae	3	9	119 ± 20.6	17.5 ± .9	14.4 ± .9	120.7 ± 13	599 ± 60.9	120 ± 3.6	.2
TF	*Acacia richii*	Fabaceae	3	12	253 ± 5.3	6.3 ± .5	5.7 ± .2	15.7 ± 2.3	441 ± 54.6	158 ± 3.1	.36
TF	*Aglaia basiphylla*	Meliaceae	3	12	122 ± 24.9	12.7 ± 2.4	10 ± 1.2	64.7 ± 24	462 ± 136.1	101 ± 1.2	.22
TF	*Alstonia costata*	Apocynaceae	4	16	644 ± 186.6	5.4 ± .8	5.2 ± 1.2	11.7 ± 3.4	913 ± 197.6	190 ± 4.9	.21
TF	*Amaroria soulameoides*	Simaroubaceae	3	12	448 ± 39.8	8.5 ± .5	7.6 ± .6	28.7 ± 3.6	1066 ± 146.4	117 ± 3.3	.11

TF	*Astronidium confertiflorum*	Melastomataceae	3	12	823 ± 205	4.6 ± .6	4.3 ± .5	8.2 ± 2.1	978 ± 74.9	332 ± 3.1	.34
TF	*Bischofia javanica*	Phyllanthaceae	3	9	258 ± 13.4	6.5 ± .4	5.1 ± .4	16.6 ± 1.8	499 ± 55.4	65 ± 1.3	.13
TF	*Buchanania attenuata*	Anacardiaceae	4	16	261 ± 44.6	5.9 ± 1.1	5.6 ± .3	14.1 ± 5	402 ± 76.6	132 ± 2.6	.33
TF	*Calophyllum vitiense*	Calophyllaceae	2	8	168 ± 1.3	8.6 ± .1	9.7 ± .1	29.4 ± .4	346 ± 9	121 ± 1.4	.35
TF	*Dillenia biflora*	Dilleniaceae	6	24	188 ± 30.9	8.8 ± .4	7.6 ± .7	30.8 ± 3.1	474 ± 102.2	130 ± 5.3	.27
TF	*Fagraea gracilipes*	Gentianaceae	3	11	183 ± 56.4	8 ± .8	7.5 ± .5	25.1 ± 4.8	388 ± 120.5	185 ± 2.6	.48
TF	*Ficus barclayana*	Moraceae	3	12	490 ± 70	6.5 ± .5	6.5 ± .9	16.9 ± 2.5	828 ± 84.5	155 ± 2.2	.19
TF	*Ficus fulvopilosa*	Moraceae	3	11	645 ± 45.7	4.9 ± .7	5.7 ± 1	9.4 ± 2.7	732 ± 99.1	332 ± 2.7	.45
TF	*Flacourtia vitiensis*	Salicaceae	3	12	419 ± 51.8	5.2 ± .7	7.2 ± .5	10.8 ± 2.9	447 ± 76.4	86 ± 1.7	.19
TF	*Ixora maxima*	Rubiaceae	3	12	231 ± 41.7	7.4 ± 1	8.1 ± .1	21.8 ± 6.2	423 ± 145.3	173 ± 2.6	.41
TF	*Maesa tabacifolia*	Primulaceae	3	10	312 ± 27.5	5.3 ± .7	5.7 ± .2	11.1 ± 3.2	402 ± 68.3	192 ± 2.8	.48
TF	*Micromelum minutum*	Rutaceae	3	12	320 ± 57.5	5.4 ± .4	6.5 ± .3	11.7 ± 1.8	405 ± 108.7	141 ± 4.4	.35
TF	*Neuburgia corynocarpa*	Loganiaceae	3	12	190 ± 15.7	8.5 ± .8	9.1 ± 2	28.8 ± 5.4	402 ± 46.7	116 ± 2.7	.29
TF	*Nothobaccaurea pulvinata*	Phyllanthaceae	4	13	156 ± 25	7.1 ± .3	8 ± .6	20 ± 1.7	266 ± 41.6	116 ± 1.4	.43
TF	*Polyscias multijuga*	Araliaceae	2	8	277 ± 35.4	4.1 ± .1	3.3 ± 2.8	6.7 ± .4	261 ± 20.7	68 ± 1.2	.26
TF	*Tabernaemontana pandacaqui*	Apocynaceae	3	12	551 ± 99.3	4.9 ± .8	4.7 ± .2	9.5 ± 3	713 ± 200.1	169 ± 3.5	.24
TF	*Tabernaemontana thurstonii*	Apocynaceae	3	6	150 ± 35.7	8.1 ± .3	6.9 ± .4	26.1 ± 2.1	350 ± 93.7	158 ± 1.2	.45
TF	*Vavaea amicorum*	Meliaceae	3	12	272 ± 46.9	6.4 ± .3	6.3 ± .3	15.9 ± 1.6	451 ± 104.2	87 ± 2.5	.19
TSF	*Allophylus crassinervis*	Sapindaceae	3	12	276 ± 13	6.8 ± .8	5 ± .2	18.2 ± 4.2	580 ± 116.7	151 ± 3.3	.26
TSF	*Calophyllum brasiliense*	Calophyllaceae	4	16	211 ± 61.5	8 ± .3	11.1 ± .2	25.2 ± 1.8	347 ± 97.9	125 ± 3.6	.36
TSF	*Casearia decandra*	Salicaceae	4	14	419 ± 53.3	7 ± .6	4.4 ± .5	19.3 ± 3.2	985 ± 140.3	142 ± 4.5	.14
TSF	*Casearia sylvestris*	Salicaceae	5	13	844 ± 192	4.1 ± .3	4.5 ± .6	6.8 ± 1.1	846 ± 181.1	268 ± 3.8	.32
TSF	*Coccoloba diversifolia*	Polygonaceae	3	12	119 ± 45.3	9 ± .9	5.1 ± 0	31.9 ± 6.7	368 ± 90.3	80 ± 1.4	.22
TSF	*Comocladia glabra*	Anacardiaceae	3	12	372 ± 51.1	4.9 ± .6	4 ± .3	9.5 ± 2.2	526 ± 65.2	118 ± 2.6	.23
TSF	*Drypetes alba*	Putranjivaceae	3	12	280 ± 25.7	5.3 ± .7	5.9 ± .1	11 ± 2.9	358 ± 100.9	65 ± .9	.18
TSF	*Eugenia axillaris*	Myrtaceae	3	6	928 ± 172.7	2.9 ± .3	4.9 ± 0	3.3 ± .6	483 ± 164.7	89 ± 1.7	.19
TSF	*Eugenia biflora*	Myrtaceae	4	16	378 ± 25.9	3.8 ± .2	6.3 ± .2	5.7 ± .6	258 ± 4.4	68 ± .6	.26
TSF	*Faramea occidentalis*	Rubiaceae	3	6	238 ± 20.6	7.1 ± .3	4.4 ± .4	19.6 ± 1.9	569 ± 72.5	62 ± 2	.11
TSF	*Gonzalagunia hirsuta*	Rubiaceae	3	12	217 ± 23.6	8.6 ± .2	5.7 ± .2	29 ± 1	613 ± 68.4	229 ± 2.4	.37
TSF	*Malpighia coccigera*	Malpighiaceae	4	14	293 ± 19.5	7.4 ± .3	4.7 ± .1	21.4 ± 1.9	726 ± 93.5	191 ± 1.4	.26
TSF	*Miconia prasina*	Melastomataceae	3	12	676 ± 69.4	3.2 ± .6	3.4 ± .5	4.2 ± 1.4	550 ± 187.7	119 ± 4.1	.22
TSF	*Neea buxifolia*	Nyctaginaceae	3	11	249 ± 50.9	7.2 ± 0	8.3 ± .5	20.3 ± .1	419 ± 72.5	35 ± 1.6	.08
TSF	*Psidium amplexicaule*	Myrtaceae	3	12	420 ± 47.3	3.7 ± .6	5.1 ± .3	5.4 ± 1.7	325 ± 100.6	105 ± 3.2	.32
TSF	*Psychotria nervosa*	Rubiaceae	3	12	104 ± 20	9.7 ± 1.5	9.7 ± 3.3	37.4 ± 12	261 ± 40.1	70 ± 1.1	.27
TSF	*Randia aculeata*	Rubiaceae	3	11	210 ± 15.4	8.2 ± .4	6.6 ± 1	26.2 ± 2.4	510 ± 104.8	130 ± 1.5	.25
TSF	*Rondeletia inermis*	Rubiaceae	4	16	195 ± 23.2	8.2 ± .6	5.9 ± .3	26.8 ± 3.9	505 ± 49.9	107 ± 3	.21
TSF	*Schefflera morototoni*	Araliaceae	3	12	260 ± 56.6	6.5 ± .8	4.4 ± .8	16.6 ± 4.2	562 ± 203.9	100 ± 3.1	.18
TSF	*Stenostomum resinosum*	Rubiaceae	3	12	224 ± 39.5	7.2 ± 1.4	6.6 ± 1.1	20.9 ± 8	433 ± 106.6	88 ± 2.3	.2
TSF	*Thouinia striata*	Sapindaceae	3	12	602 ± 142.8	4.2 ± .3	4.2 ± .3	7 ± 1.1	663 ± 195.3	152 ± 6.7	.23

Note. BF = boreal forest, TRF = temperate rain forest, TF = tropical rain forest, TSF = tropical seasonal (moist) forest, g_{op} = operational stomatal conductance, pa_{max} = maximum stomatal pore area, g_{max} = theoretical maximum stomatal conductance, leaves (n) = number of leaves used for the calculation of mean g_{max}, and g_{op} (n) = number of g_{op} measurements on the same leaves for calculation of mean g_{op} (mean g_{op} values are weighted mean values). All errors are standard deviation.

where n species g_{op} is the total number of individual g_{op} measurements per species, n biome g_{op} is the total number of species g_{op} measurements for a given biome, and species g_{op} is the mean g_{op} for a given species. The $g_{op}:g_{max}$ ratios were thus calculated from the weighted mean g_{op} and mean g_{max} values (weighted g_{op}/g_{max}). Normality tests (Shapiro-Wilk W-test and Anderson-Darling A-test) and post hoc tests (Levene's test for homogeneity of variance from means, Tukey's honest significant difference test for normal data, and the Kruskal-Wallis test for equal medians for nonnormal data) were carried out as necessary on all data and data groups. Reduced major axis (RMA) regressions were performed to investigate the relationship between g_{op} and g_{max} and to determine r^2 and statistical significance ($P < 0.05$). Boxplots were generated to determine data distribution and differences between groups. All statistical analyses were performed using Past version 3.14 (http://folk.uio.no/ohammer/past/). Figures were generated using R statistical package version 3 (R Core Team 2015).

Results

The $g_{op}:g_{max}$ Ratio across Biomes

Overall, across 74 species and four biomes, the $g_{op}:g_{max}$ ratio was 0.26 (see table 2 for a comparison of recent investigations into the $g_{op}:g_{max}$ ratio). The tropical seasonal (moist) forest displayed the smallest mean $g_{op}:g_{max}$ ratio (0.23), while the highest $g_{op}:g_{max}$ ratio was found in the tropical rain forest (0.31; table 1). High variability in species-level $g_{op}:g_{max}$ ratio was observed between species within and across all biomes, from a minimum 0.08 in *Neea buxifolia* from the tropical seasonal (moist) forest to a maximum 0.6 in *Sambucus racemosa* from the boreal forest (table 1). There was no significant difference in median biome $g_{op}:g_{max}$ ratios $\chi^2 = 4.976$, $P = 0.17$) with mean and median values among biomes in close agreement (fig. 1*A*; tables 3, S2).

The $g_{op}:g_{max}$ Ratio in Habitat Groups

Species data were categorized according to two habitat groups: open canopy and understory subcanopy. Overall, the biome-wide mean $g_{op}:g_{max}$ ratio in both the open-canopy ($n = 26$) and the understory-subcanopy ($n = 49$) habitats was the same, with a calculated ratio of 0.28 ($P = 0.319$; fig. 1; tables 3, S3).

In the open-canopy habitat, there was no significant difference in overall mean $g_{op}:g_{max}$ ratio between biomes ($F = 0.157$, $P = 0.924$; fig. 1; table S4). In the understory-subcanopy habitat, there was a significant difference in mean $g_{op}:g_{max}$ ratio between the tropical rain forest and both the temperate rain forest and the tropical seasonal (moist) forest biomes ($P = 0.005$ and $P = 0.026$, respectively; Tukey's honest significant difference test), with the tropical rain forest displaying the highest mean $g_{op}:g_{max}$ ratio in both habitats across all biomes at 0.32 (fig. 1; table S5).

In the boreal forest, tropical seasonal (moist) forest, and tropical rain forest, there was no significant difference between the mean $g_{op}:g_{max}$ ratio of the open-canopy habitat and that of the understory-subcanopy habitat ($P > 0.05$; fig. 2). Only the temperate rain forest displayed a significant difference between habitat groups ($F = 6.692$, $P = 0.02$).

The $g_{op}:g_{max}$ Ratio in Growth Habit Groups

Species data were also categorized according to plant growth habit (tree and shrub) within each biome. The overall mean $g_{op}:g_{max}$ ratio was 0.25 for shrubs ($n = 34$) and 0.27 for trees ($n = 41$; table S6). Overall, there was no significant difference in the $g_{op}:g_{max}$ ratio between shrub and tree growth habits $\chi^2 = 0.509$, $P = 0.476$; table S6).

No significant difference was observed in either the mean shrub $g_{op}:g_{max}$ ratio or the mean tree $g_{op}:g_{max}$ ratio between biomes (ANOVA $P = 0.2789$ and Kruskal-Wallis $\chi^2 = 3.768$, $P = 0.288$, respectively; fig. 1*C*; tables 3, S7). Within biomes, there was no statistically significant difference between mean/median shrub and tree $g_{op}:g_{max}$ ratios ($P > 0.05$).

Relationship between g_{op} and g_{max}

Linear regressions were performed using RMA to account for errors in both x and y variables. Across the total 75 C_3 woody angiosperm species and four biomes, the best-fit linear relationship between g_{op} and g_{max} was $g_{op} = 0.26 \cdot g_{max} - 5.56$ ($r^2 = 0.304$, $P < 0.001$; table 3; fig. 1). Within each of the four study biomes, there was a significant positive relationship between g_{op} and g_{max}, with no significant difference between slopes $\chi^2 = 5.375$, $P = 0.146$; table 3; fig. 2).

Relationships between g_{op} and g_{max} in both the open-canopy and understory-subcanopy habitat groups were significant ($r^2 = 0.262$, $P = 0.009$ and $r^2 = 0.238$, $P < 0.001$, respectively; table 3; fig. 2). In both the tree and the shrub groups, the relationships between g_{op} and g_{max} were also significant ($r^2 = 0.209$, $P < 0.001$ and $r^2 = 0.318$, $P = 0.007$, respectively; table 3; fig. 2), with no difference between slopes $\chi^2 = 3.252$, $P = 0.07$; table 3). There was significant difference in the slopes of the open-canopy and understory-subcanopy habitats $\chi^2 = 3.986$, $P = 0.0459$; table 3; fig. 2).

Stomatal Traits

Stomatal density. There was wide species variation in the range of estimated D across all four biomes, from a minimum average D of ~65 mm^{-2} in the boreal forest (*S. racemosa*) to a maximum average of 928 mm^{-2} in the tropical seasonal forest (*Eugenia axillaris*; table 1). There was no statistically significant difference in mean D between boreal forest and temperate rain forest species ($P = 0.172$). There was also not a significant difference in D between the tropical rain forest and the tropical seasonal (moist) forest ($P = 0.72$). A significant difference was observed between the boreal forest and both the tropical rain forest ($P = 0.0002$) and the tropical seasonal (moist) forest ($P = 0.0004$) and, likewise, between the temperate rain forest and both the tropical rain forest and the tropical seasonal (moist) forest ($P = 0.001$ and $P = 0.002$, respectively; table 1).

Stomatal pore area. Overall, stomatal pore length ranged from a mean minimum 2.9 μm (*E. axillaris*) in the tropical seasonal (moist) forest to a mean maximum 18.1 μm (*Populus*

Table 2

Most Recent Investigations of the Relationship between Operational Stomatal Conductance (g_{op}) and Theoretical Maximum Stomatal Conductance (g_{max}) and Experiment Details, with Determined $g_{op} : g_{max}$ Ratios

Study	Study type	Plant type	Environment/protocol	Species (n)	Pore (calculated as)	$g_{op}:g_{max}$	Equation
Franks et al. 2009	Single species	Woody angiosperm (*Eucalyptus globulus* seedlings and coppice shoots)	Field experiment	1	Circle	.2	$g_{w\,max} = (d \cdot D \cdot a_{max})/(v \cdot (l + (\pi/2) \cdot \sqrt{(a_{max}/\pi)}))$
Dow et al. 2014	Single species	Herbaceous (*Arabidopsis thaliana* mature rosette leaves)	Growth chamber	1 (6 genotypes)	Ellipse	.2	Anatomical $g_{s\,max} = (d \cdot D \cdot a_{max})/(v \cdot (l + (\pi/2) \cdot \sqrt{(a_{max}/\pi)}))$
Franks et al. 2014	Theoretical model	…	…	…	Circle	.2	$g_{w\,max} = (d \cdot D \cdot a_{max})/(v \cdot (l + (\pi/2) \cdot \sqrt{(a_{max}/\pi)}))$
McElwain et al. 2016*b*	Multispecies	Mixed phylogenies: angiosperm (woody and herbaceous); gymnosperm (conifer and cycad)	Glasshouse and growth chamber	18	Ellipse	.25	$g_{max} = \frac{(d_w/v) \cdot D \cdot pa_{max}}{pd + (\pi/2) \cdot \sqrt{(pa_{max}/\pi)}}$
Murray et al. 2019	Multispecies, multibiome	Woody angiosperms (evergreen and deciduous)	Natural (variance protocol)	74	Ellipse	.26	$g_{max} = \frac{(d_w/v) \cdot D \cdot pa_{max}}{pd + (\pi/2) \cdot \sqrt{(pa_{max}/\pi)}}$

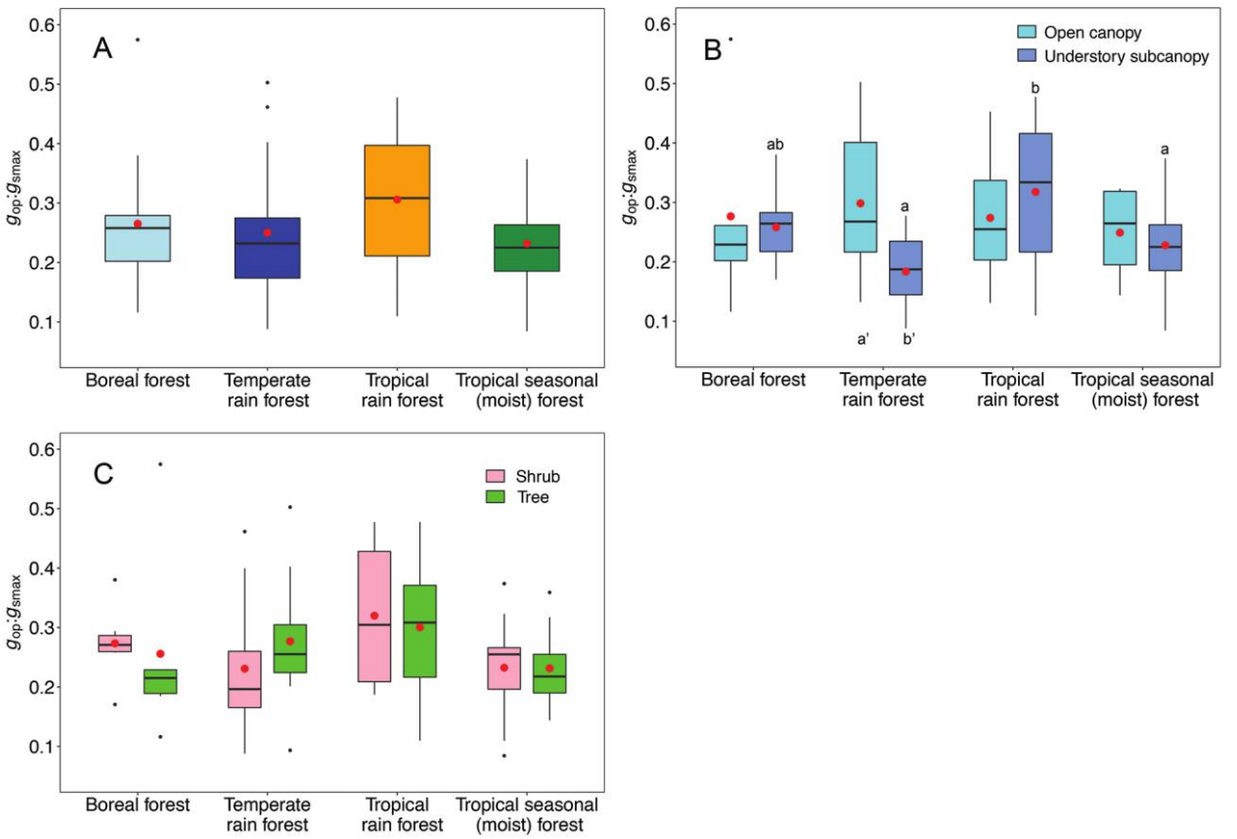

Fig. 1 Boxplots showing the ratio of operational stomatal conductance to theoretical maximum stomatal conductance (g_{op}:g_{max}) for biomes (*A*), habitats (*B*), and plant growth habits (*C*). Boxes represent the interquartile range (IQR), horizontal lines within the boxes represent medians, red circles represent means, whiskers extend to 1.5 times the IQR, and black circles are outliers. In *B*, letters above boxplots indicate pairwise comparison for the understory-subcanopy habitat across biomes (Tukey's honest significant difference test), and letters below boxplots indicate significant differences in the two habitats for temperate rain forest. All other comparisons show no significant difference across or within biomes.

balsamifera) in the boreal forest. Stomatal pore length differed significantly between all biomes except between the tropical rain forest and the tropical seasonal (moist) forest, which shared the same mean and median stomatal pore length values ($P = 0.6796$). Calculated mean maximum stomatal pore area (pa_{max}) values reflected mean stomatal pore length values and ranged from a mean minimum pa_{max} of 3.3 μm^2 (*E. axillaris*) in the tropical seasonal (moist) forest to a mean maximum of ~129 μm^2 (*P. balsamifera*) in the boreal forest. There was a significant difference in pa_{max} between most biomes ($P = 3.25 \times 10^{-8}$) except

Table 3

Calculated Ratios of Operational Stomatal Conductance to Maximum Theoretical Stomatal Conductance (g_{op}:g_{max}) and Reduced Major Axis Regression Equations for the Relationship between g_{op} and g_{max} at Biome, Habitat, and Plant Growth Habit Levels

Regression level, data group	*n*	g_{op}:g_{max} ratio	g_{op}	r^2	*P*	*P* (same slope)
Overall	75	.26	$.256 \cdot g_{max} - 5.561$	.304	.000	...
Biome:						
Boreal forest	13	.27	$.155 \cdot g_{max} + 52.845$	.326	.042	$\chi^2 = 5.375$
Temperate rain forest	19	.25	$.245 \cdot g_{max} - 7.809$	.323	.011	$P = .146$
Tropical rain forest	22	.31	$.2997 \cdot g_{max} - 7.587$	.244	.019	...
Tropical seasonal forest	21	.23	$.309 \cdot g_{max} - 41.366$	.463	.001	...
Habitat:						
Open canopy	26	.28	$.265 \cdot g_{max} - 2.603$	.262	.009	$\chi^2 = 3.986$
Understory subcanopy	49	.25	$.310 \cdot g_{max} - 24.222$	.238	.000	$P = .046$
Plant habit:						
Tree	41	.27	$.222 \cdot g_{max} + 17.237$	.318	.000	$\chi^2 = 3.252$
Shrub	34	.26	$.323 \cdot g_{max} - 40.385$	.209	.007	$P = .071$

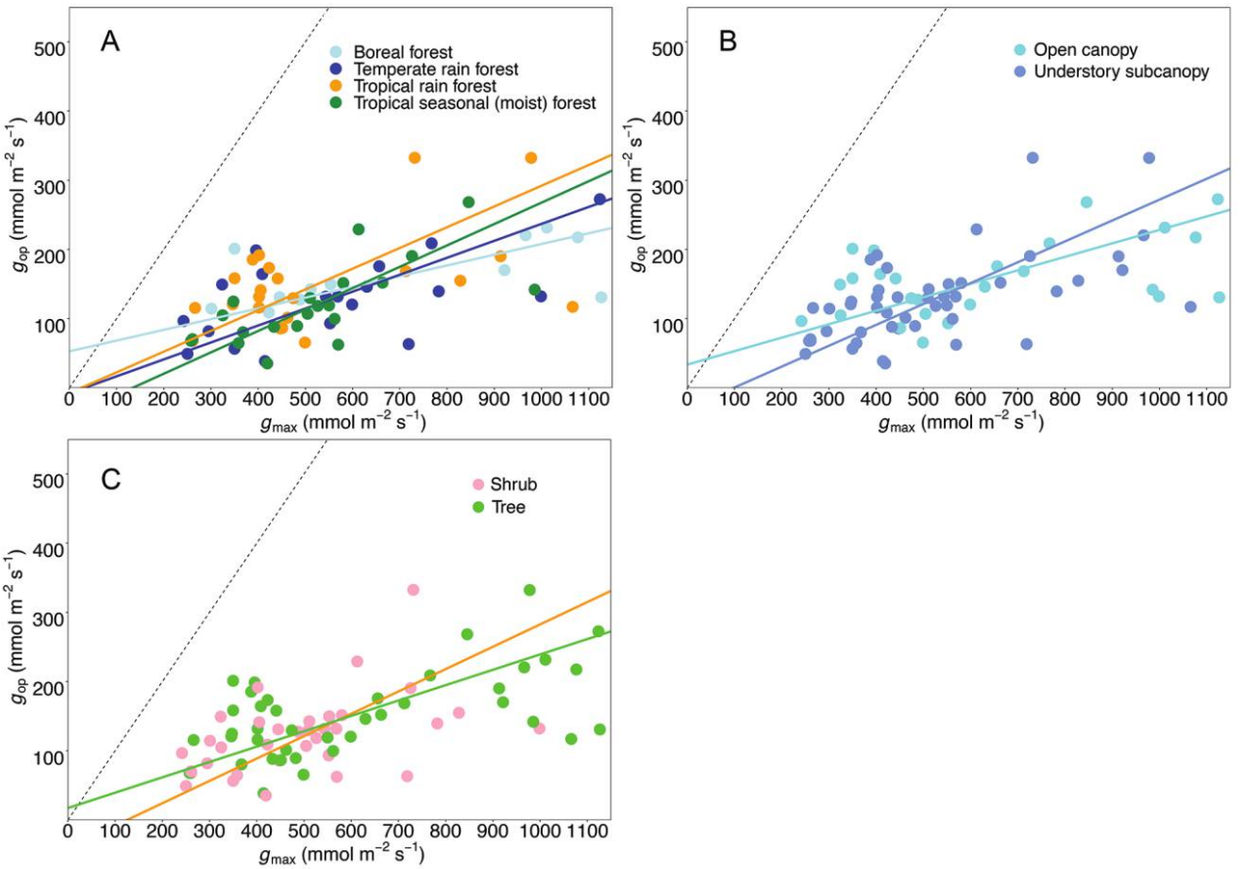

Fig. 2 Scatterplots showing the scaling relationship between species' averaged operational stomatal conductance (g_{op}) and maximum theoretical stomatal conductance (g_{max}) of C_3 woody angiosperms for biomes (*A*), habitats (*B*), and plant growth habits (*C*). Lines corresponding to the legend color are the fitted reduced major axis regressions. The dashed line is the 1:1 relationship (refer to table 3 for the regression equations and *P* values). Only in *C* is there significant difference in slope between shrub and tree, but all other comparisons in *A* and *B* show no significant difference in slopes ($P < 0.05$).

between the tropical rain forest and the tropical seasonal (moist) forest where there was no significant difference ($P = 0.51$).

Relationship between Anatomical Measurements and Calculated g_{max}

A significant strong relationship between g_{max} and D was found among tropical rain forest taxa ($g_{max} = 1.2185 \cdot D + 121.91$; $r^2 = 0.684$, $P < 0.0001$), and a moderately strong and significant relationship between g_{max} and D was found in the temperate rain forest ($g_{max} = 3.7912 \cdot D - 122.01$; $r^2 = 0.518$, $P = 0.001$; fig. 3). No significant relationship between g_{max} and D was observed in either the boreal forest ($g_{max} = 3.526 \cdot D + 176.87$; $r^2 = 0.009$, $P = 0.77$) or the tropical seasonal (moist) forest ($g_{max} = 0.817 \cdot D + 226.13$; $r^2 = 0.15$, $P = 0.085$; fig. 3). Overall, when all taxa from all biomes were lumped together, no relationship was evident. There was no difference in slopes between the boreal forest and the temperate rain forest or between the tropical rain forest and the tropical seasonal (moist) forest ($P = 0.84$ and $P = 0.113$; fig. 3).

There was a moderately strong but significant relationship between g_{max} and pa_{max} in the boreal forest ($g_{max} = 7.439 \cdot pa_{max} + 46.884$; $r^2 = 0.452$, $P = 0.012$); however, no relationship between g_{max} and pa_{max} was established in the other biomes: temperate rain forest ($r^2 = 0.073$, $P = 0.262$), tropical rain forest ($r^2 = 0.022$, $P = 0.508$), and tropical seasonal (moist) forest ($r^2 = 0.0192$, $P = 0.55$; fig. 3). There was no difference in slopes between the boreal forest and the temperate rain forest or between the tropical rain forest and the tropical seasonal (moist) forest ($P = 0.56$ and $P = 0.99$, respectively; fig. 3).

Relationship of g_{max} to Environmental Data

Correlation regressions between all species' g_{max}, g_{op}, and g_{op}:g_{max} ratios and environmental variables of temperature, PAR, and VPD showed no significant relationships (fig. S1, available online).

Discussion

g_{op}:g_{max} Ratios and Relationships

We find a consistent relationship between theoretical g_{max} calculated from stomatal anatomy and field-measured g_{op},

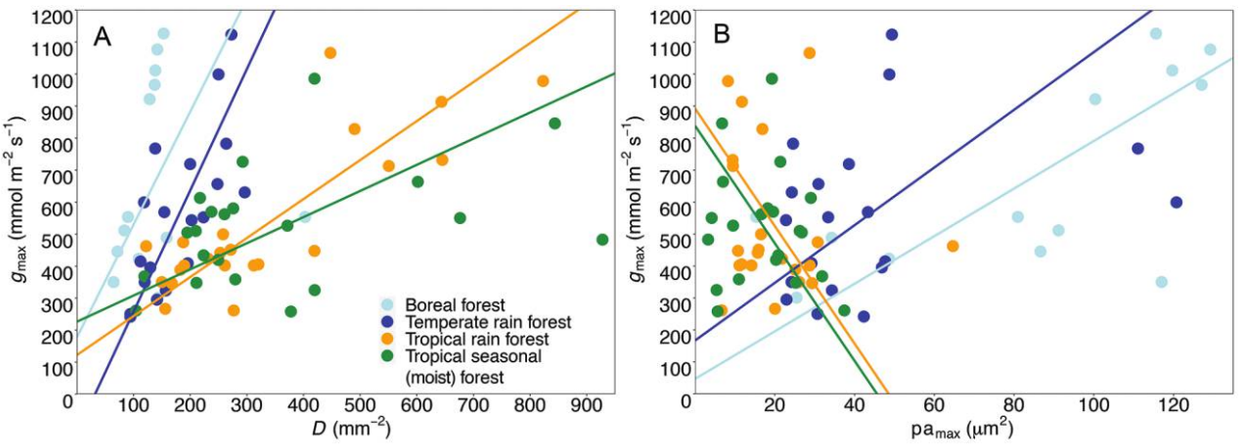

Fig. 3 Scatterplots of theoretical maximum stomatal conductance (g_{max}) and stomatal density (D; *A*) and maximum stomatal pore area (pa_{max}; *B*) for biomes. Lines corresponding to the legend color are the fitted reduced major axis regressions. In both *A* and *B*, there are no significant differences in relationships between the boreal forest and the temperate rain forest (D: $P = 0.84$; pa_{max}: $P = 0.56$, respectively) or between the tropical rain forest and the tropical seasonal (moist) forest (D: $P = 0.11$; pa_{max}: $P = 0.99$, respectively).

with an overall mean $g_{op}:g_{max}$ ratio of 0.26. At the biome level, woody angiosperm species in the field tend to operate between 23% and 31% of their calculated g_{max}, which is in good agreement with previous, but less taxonomically extensive (~15 species), studies in a mix of glasshouse, chamber, and field experiments (Franks et al. 2009, 2014; Dow and Bergmann 2014; McElwain et al. 2016*b*; see table 3 for the most recent studies). This is significant, considering the diversity in species and climate/environments covered in this study and between all studies to date. It confirms the existence of an apparent ideal $g_{op}:g_{max}$ ratio, as was suggested in previous studies (Dow et al. 2014; Franks et al. 2014; McElwain et al. 2016*b*). The wide-ranging interspecific variation in $g_{op}:g_{max}$ ratios we observed (between 0.08 and 0.57) is also consistent with reported maximum $g_{op}:g_{max}$ ratios of between 0.15 and 0.98 across species using a variance protocol (McElwain et al. 2016*b*). Despite such wide-ranging $g_{op}:g_{max}$ ratios across species within each biome, no statistical difference between overall biome-level $g_{op}:g_{max}$ ratios was observed.

Habitat Groups

This pattern of consistency in the $g_{op}:g_{max}$ ratio was also noted in two habitat groups: open canopy and understory subcanopy. Considering the different environmental conditions experienced by plants in these two habitats, including lower PAR and VPD values exhibited in the understory-subcanopy habitat than in the open-canopy habitat, as well as lower g_{op} demonstrated by the understory-subcanopy plants (Murray et al. 2019), the consistency in the $g_{op}:g_{op}$ ratio between these two habitats is noteworthy. It is surely interesting that such consistency has emerged from this study despite high environment-driven species variability in each and further supports the theory that plants operate at an ideal $g_{op}:g_{max}$ ratio.

Plant Growth Habit

The $g_{op}:g_{max}$ ratio was again demonstrated between tree and shrub plant growth habits. Previous studies have investigated in total around 20 different species comprising different growth habits, including herbaceous plants, woody shrubs, and trees (table 3). It is not clear from these studies, however, whether growth habit had any influence on the $g_{op}:g_{max}$ ratio. This study of 33 shrub and 42 tree species determined that growth habit does not appear to have any influence on overall $g_{op}:g_{max}$ ratio. This once again reinforces our discovery of a consistent macrolevel $g_{op}:g_{max}$ ratio.

Stomatal Morphological Traits

In the cool higher-latitude biomes of the boreal forest and the temperate rain forest, stomatal pore size influences g_{max} to the greatest extent (fig. 3*B*). On the other hand, in the warmer biomes of the tropical rain forest and the tropical seasonal forest, this is not the case, and stomatal density is most influential in these biomes (fig. 3*A*). The much larger pore size observed in the boreal forest may reflect greater overall genome size in the boreal biome taxa than in the other biomes, as guard cell size frequently scales with genome size (Beaulieu et al. 2008). Our results may reflect the pressures that climate exerts on leaf stomatal development in each biome. For instance, in the hotter biomes, which require greater evaporative cooling, this is clearly attained via higher D and smaller stomata (fig. 3): smaller stomata have been observed to respond more rapidly to environmental stimuli (Drake et al. 2013). Our results from the tropical rain forest corroborate findings in *Eucalyptus globulus*, in which higher rates of gas exchange were achieved by a greater density of small stomata (Franks et al. 2009). The opposite is true for the most northern latitude biomes, where fewer larger stomata ensure high

g_{max} to exploit the short window of opportunity for carbon gain experienced in the boreal forest.

Species-Level Variability in the g_{op}:g_{max} Ratio

In competition and in association with neighboring species, plants can optimize physiological processes, such as stomatal conductance, toward proper growth, development, and reproduction; this results in their occupying a particular niche space (Sterck et al. 2011; McElwain et al. 2016*b*). This might account for the diversity of species-specific g_{op}:g_{max} ratios that we find within each biome investigated here. While a single species experiment in the "natural" environment may yield a low g_{op}:g_{max} ratio, such a monocultural ecosystem may function very differently from the truly natural environment of very mixed vegetation types in unmanaged forests. From our results, such ecosystems yield widely diverging species g_{op}:g_{max} ratios, which may also be constantly changing in dynamic response to environmental fluxes. The minimum g_{op}:g_{max} ratio we observed in our study was 0.08 (*Neea buxifolia*) in the tropical seasonal (moist) forest, and the highest value was 0.57 (*Sambucus racemosa*) in the boreal forest. Despite wide species-level variability, however, at the biome level, the average g_{op}:g_{max} ratio is highly consistent across all four biomes investigated. The variety of stomatal density and size combinations among species appears to facilitate each species' g_{max} requirements in response to localized community composition and microenvironmental fluxes (Franks and Beerling 2009) and, perhaps, enables the coexistence of diverse species (McElwain et al. 2016), as in the tropical rain forest.

The g_{op}:g_{max} data presented here is a broad representation of C_3 woody angiosperm species common within each biome (Murray et al. 2019). We set out to investigate the nature of the relationship between g_{op} and g_{max} in as many biome-representative species as possible within the limits of the study; however, a complete picture of g_{op} may not have been captured, since it was not possible to measure the diurnal courses of g_{op} for every measured leaf. Nonetheless, despite these limits to our sampling and the wide interspecies variability in the relationship between g_{op} and g_{max}, there is consistency in the g_{op}:g_{max} ratio across biomes, habitats, and growth habits presented here, providing an important new reference for studies at the biome, habitat, and growth habit levels of woody angiosperm species of unknown g_{op}:g_{max} ratio in the natural environment. A potential future study might incorporate relative abundance data to quantify a community-weighted g_{op}:g_{max} ratio to further understand whether there is any departure from the g_{op}:g_{max} ratio so far observed.

Conclusion

Until now, there were few reference points for the relationship between g_{op} and g_{max} and no studies in natural ecosystems. This study using the variance protocol (McElwain et al. 2016*b*; Murray et al. 2019) presents in one data set the g_{op}:g_{max} ratios of 74 woody angiosperm species in their natural habitats from across four biomes. We have shown compelling evidence for consistency in the ratio between physiological g_{op} and anatomical g_{max} among biome-representative woody angiosperms at the levels of biome, habitat, and plant growth habit. This new data set provides a valuable contemporary calibration reference for woody angiosperms in vegetation-climate and paleoclimate models. For paleobotanists striving to understand plant macroevolutionary patterns and paleoecophysiological function from measurable fossil traits (Franks et al. 2014; McElwain et al. 2016*a*) where no modern equivalents exist, our results now offer a valuable reference for the g_{op}:g_{max} ratio at the biome, habitat, and plant growth habit levels for woody Eudicots. In such cases, the discovery of a best estimate of the g_{op}:g_{max} ratio is a good starting point for the foundation of sound paleoclimate proxies for further understanding plants' role in mediating climate past and present. In their chapter on the capture of CO_2 by leaves and stomata, Williams et al. (2004), while conceding a large degree of uncertainty, suggested that species-level differences, though great, may not ultimately be important considering the observed conformity in g_{max} response found at the PFT level (Williams et al. 2004). We argue the same for the relationship between g_{op} and g_{max}: while there is almost the full breadth of disparity among species, at the levels of growth habit, habitat, and biome, the relationship is consistent.

Acknowledgments

We thank research assistant Ciara Egan and student interns Marion Lestienne and Louise Flanagan for assistance with slide preparation and Amanda Porter and Crissy Evan-Fitzgerald for many discussions on anatomical g_{max}. We acknowledge University College Dublin School of Biology and Environmental Science for facilitating all lab work carried out for this project. This project was made possible by funding from a Science Foundation Ireland (SFI) Principal Investigator Award (PI) 11/PI/1103.

Literature Cited

Ainsworth EA, A Rogers 2007 The response of photosynthesis and stomatal conductance to rising [CO_2]: mechanisms and environmental interactions. Plant Cell Environ 30:258–270.

APG (Angiosperm Phylogeny Group), MW Chase, MJM Christenhusz, MF Fay, JW Byng, WS Judd, DE Soltis, et al 2016 An update of the Angiosperm Phylogeny Group classification for the orders and families of flowering plants: APG IV. Bot J Linn Soc 181:1–20.

Beaulieu JM, IJ Leitch, S Patel, A Pendharkar, CA Knight 2008 Genome size is a strong predictor of cell size and stomatal density in angiosperms. New Phytol 179:975–986.

Berry JA, DJ Beerling, PJ Franks 2010 Stomata: key players in the earth system, past and present. Curr Opin Plant Biol 13:233–240.

Betts RA, O Boucher, M Collins, PM Cox, PD Falloon, N Gedney, DL Hemming, et al 2007 Projected increase in continental runoff due to plant responses to increasing carbon dioxide. Nature 448:1037–1041.

Blonder B, V Buzzard, I Simova, L Sloat, B Boyle, R Lipson, B Aguilar-Beaucage, et al 2012 The leaf-area shrinkage effect can bias paleoclimate and ecology research. Am J Bot 99:1756–1763.

Buckley TN 2005 The control of stomata by water balance. New Phytol 168:275–292.
Buckley TN, SJ Schymanski 2014 Stomatal optimisation in relation to atmospheric CO_2. New Phytol 201:372–377.
Casson S, JE Gray 2008 Influence of environmental factors on stomatal development. New Phytol 178:9–23.
Dow GJ, DC Bergmann 2014 Patterning and processes: how stomatal development defines physiological potential. Curr Opin Plant Biol 21:67–74.
Dow GJ, DC Bergmann, JA Berry 2014 An integrated model of stomatal development and leaf physiology. New Phytol 201:1218–1226.
Drake PL, RH Froend, PJ Franks 2013 Smaller, faster stomata: scaling of stomatal size, rate of response, and stomatal conductance. J Exp Bot 64:495–505.
Engineer CB, M Hashimoto-Sugimoto, J Negi, M Israelsson-Nordström, T Azoulay-Shemer, WJ Rappel, K Iba, JI Schroeder 2016 CO_2 sensing and CO_2 regulation of stomatal conductance: advances and open questions. Trends Plant Sci 21:16–30.
Farquhar GD, TD Sharkey 1982 Stomatal conductance and photosynthesis. Annu Rev Plant Physiol 33:317–345. https://doi.org/10.1146/annurev.pp.33.060182.001533.
Franks PJ, MA Adams, JS Amthor, MM Barbour, JA Berry, DS Ellsworth, GD Farquhar, et al 2013 Sensitivity of plants to changing atmospheric CO_2 concentration: from the geological past to the next century. New Phytol 197:1077–1094.
Franks PJ, DJ Beerling 2009 Maximum leaf conductance driven by CO_2 effects on stomatal size and density over geologic time. Proc Natl Acad Sci USA 106:10343–10347.
Franks PJ, TW Doheny-Adams, ZJ Britton-Harper, JE Gray 2015 Increasing water-use efficiency directly through genetic manipulation of stomatal density. New Phytol 207:188–195.
Franks PJ, PL Drake, DJ Beerling 2009 Plasticity in maximum stomatal conductance constrained by negative correlation between stomatal size and density: an analysis using *Eucalyptus globulus*. Plant Cell Environ 32:1737–1748. https://doi.org/10.1111/j.1365-3040.2009.002031.x.
Franks PJ, IJ Leitch, EM Ruszala, AM Hetherington, DJ Beerling 2012 Physiological framework for adaptation of stomata to CO_2 from glacial to future concentrations. Philos Trans R Soc B 367:537–546.
Franks PJ, DL Royer, DJ Beerling, PK van de Water, DJ Cantrill, MM Barbour, JA Berry 2014 New constraints on atmospheric CO_2 concentration for the Phanerozoic. Geophys Res Lett 41:4685–4694. https://doi.org/10.1002/2014GL060457.
Gedney N, PM Cox, RA Betts, O Boucher, C Huntingford, PA Stott 2006 Detection of a direct carbon dioxide effect in continental river runoff records. Nature 439:835–838.
Gray SB, O Dermody, SP Klein, AM Locke, JM Mcgrath, RE Paul, DM Rosenthal, et al 2016 Intensifying drought eliminates the expected benefits of elevated carbon dioxide for soybean. Nat Plants 2:16132.
Haworth M, C Elliott-Kingston, JC McElwain 2013 Co-ordination of physiological and morphological responses of stomata to elevated [CO_2] in vascular plants. Oecologia 171:71–82.
Hetherington AM, FI Woodward 2003 The role of stomata in sensing and driving environmental change. Nature 424:901–908.
Hutjes RWA, P Kabat, SW Running, WJ Shuttleworth, C Field, B Bass, MF da Silva Dias, et al 1998 Biospheric aspects of the hydrological cycle. J Hydrol 212/213:1–21. https://doi.org/10.1016/S0022-1694(98)00255-8.
Katul G, S Manzoni, S Palmroth, R Oren 2009 A stomatal optimization theory to describe the effects of atmospheric CO_2 on leaf photosynthesis and transpiration. Ann Bot 105:431–442. https://doi.org/10.1093/aob/mcp292.
Katul GG, R Oren, S Manzoni, C Higgins, MB Parlange 2012 Evapotranspiration: a process driving mass transport and energy exchange in the soil-plant-atmosphere-climate system. Rev Geophys 50:RG3002. https://doi.org/10.1029/2011RG000366.
Keenan TF, J Gray, MA Friedl, M Toomey, G Bohrer, DY Hollinger, JW Munger, et al 2014 Net carbon uptake has increased through warming-induced changes in temperate forest phenology. Nat Clim Chang 4:598–604. https://doi.org/10.1038/nclimate2253.
Kollist H, M Nuhkat, MRG Roelfsema 2014 Closing gaps: linking elements that control stomatal movement. New Phytol 203:44–62.
Körner C 1995 Leaf diffusive conductances in the major vegetation types of the globe. Pages 463–490 *in* ED Schulze, MM Caldwell, eds. Ecophysiology of photosynthesis. Springer, Berlin. https://doi.org/10.1007/978-3-642-79354-7.
Lake JA, WP Quick, DJ Beerling, FI Woodward 2001 Signals from mature to new leaves. Nature 411:154.
Lammertsma EI, HJ de Boer, SC Dekker, DL Dilcher, AF Lotter, F Wagner-Cremer 2011 Global CO_2 rise leads to reduced maximum stomatal conductance in Florida vegetation. Proc Natl Acad Sci USA 108:4035–4040.
Lawson T, MR Blatt 2014 Stomatal size, speed, and responsiveness impact on photosynthesis and water use efficiency. Plant Physiol 164:1556–1570.
Lawson T, W James, J Weyers 1998 A surrogate measure of stomatal aperture. J Exp Bot 49:1397–1403.
Lawson T, JI Morison 2004 Stomatal function and physiology. Pages 217–242 *in* AR Hemsley, I Poole, eds. The evolution of plant physiology: from whole plants to ecosystem. Elsevier, Cambridge.
Leakey ADB, EA Ainsworth, CJ Bernacchi, A Rogers, SP Long, DR Ort 2009 Elevated CO_2 effects on plant carbon, nitrogen, and water relations: six important lessons from FACE. J Exp Bot 60:2859–2876. https://doi.org/10.1093/jxb/erp096.
Li Z, Y Chen, Y Wang, G Fang 2016 Dynamic changes in terrestrial net primary production and their effects on evapotranspiration. Hydrol Earth Syst Sci 20:2169–2178.
Lin Y-S, BE Medlyn, RA Duursma, IC Prentice, H Wang, S Baig, D Eamus, et al 2015 Optimal stomatal behaviour around the world. Nat Clim Chang 5:459–464.
Lomax BH, FI Woodward, IJ Leitch, CA Knight, JA Lake 2009 Genome size as a predictor of guard cell length in *Arabidopsis thaliana* is independent of environmental conditions. New Phytol 181:311–314.
Manzoni S, G Vico, G Katul, PA Fay, W Polley, S Palmroth, A Porporato 2011 Optimizing stomatal conductance for maximum carbon gain under water stress: a meta-analysis across plant functional types and climates. Funct Ecol 25:456–467. https://doi.org/10.1111/j.1365-2435.2010.01822.x.
McAusland L, S Vialet-Chabrand, P Davey, NR Baker, O Brendel, T Lawson 2016 Effects of kinetics of light-induced stomatal responses on photosynthesis and water-use efficiency. New Phytol 211:1209–1220.
McElwain JC, WG Chaloner 1995 Stomatal density and index of fossil plants track atmospheric carbon dioxide in the Palaeozoic. Ann Bot 76:389–395. https://doi.org/10.1006/anbo.1995.1112.
McElwain JC, IP Montañez, JD White, JP Wilson, C Yiotis 2016*a* Was atmospheric CO_2 capped at 1000 ppm over the past 300 million years? Palaeogeogr Palaeoclimatol Palaeoecol 441:653–658. https://doi.org/10.1016/j.palaeo.2015.10.017.
McElwain JC, C Yiotis, T Lawson 2016*b* Using modern plant trait relationships between observed and theoretical maximum stomatal conductance and vein density to examine patterns of plant macroevolution. New Phytol 209:94–103.
Medlyn BE, RA Duursma, D Eamus, DS Ellsworth, IC Prentice, CVM Barton, KY Crous, P De Angelis, M Freeman, L Wingate 2011 Reconciling the optimal and empirical approaches to modelling stomatal conductance. Glob Chang Biol 17:2134–2144.
Mott KA 2009 Opinion: stomatal responses to light and CO_2 depend on the mesophyll. Plant Cell Environ 32:1479–1486.
Murray M, WK Soh, C Yiotis, S Batke, AC Parnell, RA Spicer, T Lawson, et al 2019 Convergence in maximum stomatal conductance

of C_3 woody angiosperms in natural ecosystems across bioclimatic zones. Front Plant Sci 10:558.
Parlange JY, PE Waggoner 1970 Stomatal dimensions and resistance to diffusion. Plant Physiol 46:337–342.
Poole I, WM Kürschner 1999 Stomatal density and index: the practice. Pages 257–260 *in* TP Jones, NP Rowe, eds. Fossil plants and spores: modern techniques. Geological Society, London.
R Core Team 2015 R: a language and environment for statistical computing. R Foundation for Statistical Computing, Vienna.
Sack L, TN Buckley 2016 The developmental basis of stomatal density and flux. Plant Physiol 171:2358–2363.
Schlesinger WH, S Jasechko 2014 Transpiration in the global water cycle. Agric For Meteorol 189/190:115–117.
Schulze ED, FM Kelliher, C Körner, J Lloyd, R Leuning 1994 Relationships among maximum stomatal conductance, ecosystem surface conductance, carbon assimilation rate, and plant nitrogen nutrition: a global ecology scaling exercise. Annu Rev Ecol Syst 25:629–660.
Sterck F, L Markesteijn, F Schieving, L Poorter 2011 Functional traits determine trade-offs and niches in a tropical forest community. Proc Natl Acad Sci USA 108:20627–20632.
Ukkola AM, IC Prentice, TF Keenan, AIJM van Dijk, NR Viney, RB Myneni, J Bi 2015 Reduced streamflow in water-stressed climates consistent with CO_2 effects on vegetation. Nat Clim Chang 6:75–78.
Wagner F, R Below, PD Klerk, DL Dilcher, H Joosten, WM Kürschner, H Visscher 1996 A natural experiment on plant acclimation: lifetime stomatal frequency response of an individual tree to annual atmospheric CO_2. Proc Natl Acad Sci USA 93:11705–11708.
Williams M, FI Woodward, DD Baldocchi, D Ellsworth 2004 CO_2 capture from the leaf to the landscape. Pages 1–30 *in* WK Smith, TC Vogelmann, C Critchley, eds. Photosynthetic adaptation: chloroplast to landscape. Springer, New York.
Woodward FI 1987 Stomatal numbers are sensitive to increases in CO_2 from pre-industrial levels. Nature 327:617–618.
Woodward FI, CK Kelly 1995 The influence of CO_2 concentration on stomatal density. New Phytol 131:311–327.